Available online at www.sciencedirect.com
SCIENCE DIRECT®
Journal of Chromatography A, 1004 (2003) 131–143
JOURNAL OF CHROMATOGRAPHY A
www.elsevier.com/locate/chroma

Assessing the separation of neutral plant secondary metabolites by micellar electrokinetic chromatography

Gustavo A. Micke, Edgar P. Moraes, João P.S. Farah, Marina F.M. Tavares*
Institute of Chemistry, University of Sao Paulo, Av. Professor Lineu Prestes 748, 05508-900 Sao Paulo, SP, Brazil

Abstract

In this work, partition coefficients (P_{wm}) and solute–micelle association constants per monomer (K_m/N) were measured using micellar electrokinetic chromatography in tetraborate–sodium dodecylsulfate electrolytes for 18 important plant secondary metabolites (coumarin, verbenone, camphor, eucalyptol, carvone, α-terpineol, linalool, jasmone, bergapten, rose oxide, geraniol, *t*-anethole, citronellal, citronellol, *p*-cymene, limonene, caryophyllene and nerol) of wide occurrence in herbal extracts and essential oils. Caryophyllene presented a retention time longer than anthracene (micelle marker) and its set of constants could not be determined accurately. P_{wm} and K_m/N were generated by the non-linear data fitting of both partition and solute–micelle association models for the 17 solutes under consideration (caryophyllene excluded). P_{wm} varied from 147 (coumarin) to 13 175 (limonene) while K_m/N varied from 37 (coumarin) to 3721 (limonene). Under optimal conditions, the separation of the selected compounds was attempted successfully in commercialized samples of rose, anise and geranium essential oils.

Keywords: Association constants; Partition coefficients; Essential oils; Terpenes

1. Introduction

A milestone in the field of electrodriven separations was established in 1984 when Terabe and co-workers introduced a modified version of capillary electrophoresis, the micellar electrokinetic chromatography (MEKC) [1,2]. Through the inventive use of micellized surfactants as part of the electrolyte medium, the scope of the technique to encompass neutral compounds was extended. Since then, the versatility of the technique in handling materials from a diversity of chemical classes in complex sample matrices has been illustrated by representative applications in the clinical, forensic, environmental, and pharmaceutical areas, to name a few [2–7].

In order to design MEKC separations, a thorough understanding of the solute retention mechanism is desirable. At the present time, modeling of solute retention has been approached by the partition model in which solutes are thought to partition between two distinct phases: the pseudo-stationary phase defined by the total volume of micelles and the remaining aqueous phase. This mechanism is thus dictated by a partition coefficient, P_{wm} [8,9]. Alternatively, the interaction between solute and micelle can be described by an explicit equilibrium, in which solute and micelle are thought to combine in a defined ratio of 1:1 to form a complex entity [8]. The extent by which this association occurs is governed by the

*Corresponding author. Tel.: +55-11-3091-2056x216; fax: +55-11-3815-5579.
E-mail address: mfmtavar@iq.usp.br (M.F.M. Tavares).

0021-9673/03/$ – see front matter
doi:10.1016/S0021-9673(03)00935-X

solute–micelle association constant or binding constant, K_m, regardless whether the interaction occurs in the micelle surface or at its inner core.

The availability of association constant and/or partition coefficient data for fundamental studies or optimization purposes is still scarce in the literature for a broad number of important solutes. Foley compiled over 150 solute–micelle association constants and free solute retention factors for a variety of neutral compounds and derivatized amino acids in sodium dodecylsulfate (SDS) [9]. The author also described the usefulness of such data in the establishment of the optimal surfactant concentration for either micellar liquid chromatography (MLC) and MEKC [9,10]. Khaledi and co-workers contrasted the determination of solute–micelle binding constants by MLC and MEKC [11] studying peptides, amino acids, chlorophenols and hydrocarbons among others and initiated an extensive investigation of the migration mechanism of ionizable compounds in MEKC [3,12,13]. García et al. applied MEKC for the determination of association constants for a group of benzene derivatives and polycyclic aromatic hydrocarbons, studying the nature and concentration of several electrolytes and buffer modifiers [14]. In later work, the authors verified the correlation between retention factor and octanol–water partition coefficients [15]. More recently, Prevot et al. determined the partition coefficient of cosmetic preservatives attempting to establish a relationship between SDS partition and antimicrobial activity [16] and, Lin and Lin studied the retention characteristics of cephalosporins in cationic surfactants [17].

This work offers a contribution to the establishment of a solute–micelle interaction data base by estimating partition coefficients and solute–micelle association constants per monomer using experimentally measured retention time data derived from MEKC in tetraborate–SDS electrolytes. Several particularities of data processing and inferences on the SDS micelle structural parameters were discussed. Eighteen important plant secondary metabolites (monoterpenes, coumarins and phenylpropanoids) of wide occurrence in herbal extracts and essential oils were selected. These compounds have cosmetological importance since they are present in most personal care products (soap and toiletries) and exquisite perfumes. Moreover, they find large application in the food and drink industry as flavor enhancers and in a few cases as phytomedicines [18]. The separation of the selected compounds under optimized conditions was attempted in commercialized samples of rose, anise and geranium essential oils, offering alternative methodologies to gas chromatography, the technique of choice for monoterpenes in the fragrance and flavor industry.

2. Theory: modeling migration in MEKC for neutral solutes

Separation in MEKC can be described by a partition mechanism [8,9]:

$$[S]_{aq} \rightleftharpoons S_{MC},\ P_{wm} = \frac{[S]_{MC}}{[S]_{aq}} \tag{1}$$

where $[S]_{aq}$ and $[S]_{MC}$ are the solute concentrations in the aqueous and micellar phases, respectively, and P_{wm} is the partition coefficient.

The retention factor (k) is the product of the partition coefficient and the volume ratio of the micellar phase to the aqueous phase. The phase ratio can be written in terms of the surfactant analytical concentration (C_{SDS}), the critical micelle concentration (CMC) and the partial molar volume of surfactant ($\mathbf{V}$):

$$k = P_{wm} \cdot \frac{\mathbf{V}(C_{SDS} - CMC)}{1 - \mathbf{V}(C_{SDS} - CMC)} \tag{2}$$

Since the retention factor can be expressed by the migration time of a retained solute (t_R), a non-retained solute (t_0) and the micelle (t_{MC}), expression (2) can be rewritten as:

$$\frac{t_R - t_0}{t_0(1 - t_R/t_{MC})} = P_{wm} \cdot \frac{\mathbf{V}(C_{SDS} - CMC)}{1 - \mathbf{V}(C_{SDS} - CMC)} \tag{3}$$

An alternative model that describes the association between a solute and the micelle is known as binding or solute–micelle association model [8]. The equilibrium constant for the association process, K_m, is defined by the expression:

$$S + M \rightleftharpoons SM,\ K_m = \frac{[SM]}{[S]\,[M]} \tag{4}$$

where S is the unbound solute and [S] its equilibrium concentration; M is the free micelle of concentration [M] and SM is the aggregate solute–micelle of concentration [SM].

The effective mobility of a solute in micellar medium is given by the expression:

$$\mu_S^{eff} = \alpha\mu_{SM}^{ep} + (1-\alpha)\mu_S^{ep} \quad (5)$$

where α represents the molar fraction of solute that exists in association with the micelle and μ_{SM}^{ep} is the electrophoretic mobility of the aggregate solute–micelle; likewise $(1-\alpha)$ represents the molar fraction of solute that exists in the free form, i.e., non-associated to the micelle and μ_S^{ep} is its intrinsic electrophoretic mobility. Since the solute is neutral, μ_S^{ep} equals zero. Additionally, for small solutes, the mobility of the aggregate solute–micelle can be approximated by the mobility of the micelle, i.e., $\mu_{SM}^{ep} \cong \mu_{MC}^{ep}$.

By introducing a mass balance equation for the total concentration of micellized surfactant, the relationship between the solute effective mobility and surfactant analytical concentration can be derived:

$$\mu_S^{eff} = \frac{(C_{SDS} - CMC)\,K_m/N}{(C_{SDS} - CMC)\,K_m/N + 1} \cdot \mu_{MC}^{ep} \quad (6)$$

where N is the aggregation number.

In deriving Eq. (6), the contribution of the term [SM] for the total micelle concentration was disregarded. In practice, micelles are in a large concentration excess when compared to any of the solutes, therefore, the assumption $[M] \gg [SM]$ is expected to hold reasonably.

Eq. (6) can be rearranged in a more convenient form and expressed in terms of the experimental parameters, t_R, t_0 and t_{MC}:

$$\frac{(t_0 - t_{MC})}{(t_0 - t_R)} \cdot \frac{t_R}{t_{MC}} = 1 + \frac{N}{(C_{SDS} - CMC)\,K_m} \quad (7)$$

3. Experimental

3.1. Instrumentation

All experiments were conducted in a capillary electrophoresis system (model HP^{3D}CE, Agilent Technologies, Palo Alto, CA, USA), equipped with a diode array detector set at 200 nm, a temperature control device, maintained at 25 °C and an acquisition and treatment data software supplied by the manufacturer (HP ChemStation, rev A.06.01). A fused-silica capillary (Polymicro Technologies, Phoenix, AZ, USA) with dimensions 48.5 cm (40 cm effective length)×75 μm I.D.×365 μm O.D. was used. At the beginning of each day, the capillary was conditioned by flushing 1 mol l^{-1} NaOH solution (30 min), followed by a 20-min flush with deionized water and electrolyte solution (30 min). In between runs, the capillary was just replenished with the electrolyte (4 min). Samples and standard solutions were injected hydrodynamically (10 mbar during 3 s). The electrophoresis system was operated under normal polarity and constant voltage conditions of +20 kV. Acquisition rate was defined by a response time of 0.2 s and a peak width larger than 0.01 min.

3.2. Reagents and solutions

All reagents were of analytical grade, all solvents were of chromatographic purity and the water used to prepare the solutions was purified by deionization (Milli-Q system, Millipore, Bedford, MA, USA). Sodium dodecylsulfate (SDS) was obtained from Riedel-de-Haën (Seelze, Germany) and sodium tetraborate decahydrate was obtained from Sigma–Aldrich (St. Louis, MO, USA). Both SDS and tetraborate stock solutions were prepared in water at 100 mmol l^{-1} concentration. Working solutions consisted of mixtures of tetraborate and SDS stock solutions (pH 9.4). Specific formulations are stated in the Figure legends.

The standards anthracene, *t*-anethole, bergapten, camphor, caryophyllene, citronellal, citronellol, coumarin, *p*-cymene, geraniol, jasmone, limonene, linalool, nerol, rose oxide, α-terpineol and verbenone were purchased from Sigma–Aldrich; the standards carvone and eucalyptol were purchased form Fluka (Switzerland). Stock solutions of the standards were prepared in ethanol at 1000 mg l^{-1} concentration each and stored in freezer. Working solutions at 50 mg l^{-1} were prepared by appropriate dilution of the stocks in ethanol.

3.3. Samples

Essential oils of rose (*Rosa damascena*), anise (*Pimpinella anisum*) and geranium (*Pelargonium graveolens*) were obtained from local industries (Petite Marie Química Fina Ind. e Com. and Dierberger Óleos Essenciais, São Paulo, Brazil) and diluted in ethanol (100-fold dilution) prior to injection.

3.4. Data treatment

For the estimation of partition coefficients (P_{wm}) and solute–micelle association constants per monomer (K_m/N), a non-linear regression fitting of the experimental k and μ_S^{eff} data, separately, was conducted using the program Mac Curve Fit version 1.55, Kevin Raner Software (Australia).

4. Results and discussion

4.1. Determination of partition coefficients and association constants

For the estimation of partition coefficients and association constants, duplicate measurements of t_R for the entire set of solutes, t_0 (ethanol) and t_{MC} (anthracene), in electrolytes consisting of a fixed concentration of tetraborate (20 mmol l^{-1}, pH 9.4), and varying concentrations of SDS (from 10 to 40 mmol l^{-1}), were carried out. Besides anthracene, other dyes such as Sudan III and derivatives were tested as micelle markers. However because of practical reasons, contamination of the vial caps and electrodes due to dye adsorption, anthracene was selected as micelle marker. The concentration of tetraborate was fixed in 20 mmol l^{-1} because it offers a compromise between analysis time and resolution. The use of tetraborate as electrolyte raises a concern regarding the ability of borate to form weak complexes with hydroxyl species, altering therefore the compound overall migration. Although not confirmed experimentally, it was assumed that the compounds under investigation in this work did not undergo any complexation with borate. At least none of the compounds contains a vicinal OH moiety or is known to complex with borate.

The elution time of ethanol ($t_0 = 2.16 \pm 0.10$ min) and anthracene ($t_{MC} = 7.51 \pm 0.21$ min) remained fairly constant within the experimental error of ca. 4% for the entire range of SDS concentration. These observations suggest that variations of ionic strength from buffer to buffer preparation were not detrimental even though partition coefficients and solute–micelle association constants per monomer derived from MEKC experiments are in fact operational constants, strictly valid under the range of ionic strength of the electrolyte.

Eqs. (2) and (6) show explicitly the dependence of the retention factor or effective mobility, respectively, on the surfactant analytical concentration. In order to model solute retention by the partition model, three constants must be known, P_{wm}, **V** and CMC, whereas the modeling of solute migration by the solute–micelle association model requires the knowledge of K_m,N in addition to CMC.

Considering the dependence of CMC and N upon the surfactant structure, temperature, added electrolytes and solvents as well as pressure, use of tabulated values [19,20] of CMC and N seemed to be inappropriate to account for the particular conditions commonly used in MEKC. Therefore, as a first approach, CMC and P_{wm} (partition model, Eqs. (2) and (3); **V** was fixed at 0.246 l mol^{-1}) and CMC, N and K_m (association model, Eqs. (6) and (7)) were all estimated from the experimental data set using non-linear regression fitting.

When the partition model was considered, P_{wm} and individual values of CMC for each solute produced the best overall fitting between experimental data and the calculated retention factors. Table 1 presents the compilation of partition coefficients and corresponding CMC, illustrating the degree of hydrophobicity of the selected compounds. It is interesting to comment that a negative P_{wm} was adjusted for caryophyllene (not shown). This is related to the fact that caryophyllene is more hydrophobic than anthracene, the micelle marker, thus its migration takes longer than anthracene and it falls outside the elution window.

The preliminary treatment of the experimental data according to the solute–micelle association model produced rather odd results when CMC, N and K_m were left free to adjust. The inspection of Eq. (7) indicates an inverse relationship between N and

Table 1
Partition coefficients and solute–micelle association constants obtained in 20 mmol l^{-1} tetraborate buffers (pH 9.4) with SDS concentration varying from 10 to 40 mmol l^{-1}

Solute (retention order)	P_{wm}	CMC^{PM} (mmol l^{-1})	$r^{2\ PM}$	C_{SDS}^{opt} (mmol l^{-1})	K_m/N (l mol^{-1} monomer^{-1})	CMC^{AM} (mmol l^{-1})	$r^{2\ AM}$
Coumarin (1)	147±6	0.74±0.99	0.997	52	37±1	1.2±0.3	0.9993
Verbenone (2)	237±18	2.4±1.9	0.990	35	64±4	3.7±0.5	0.997
Camphor (3)	415±22	2.7±1.2	0.995	21	103±4	2.8±0.4	0.9986
Eucalyptol (4)	**465±12**	3.6±0.6	0.9988	**20**	110±5	3.0±0.4	0.998
Carvone (5)	**498±15**	1.6±0.8	0.998	**17**	125±3	1.8±0.3	0.9994
α-Terpineol (6)	785±48	2.3±1.5	0.994	12	186±16	1.8±0.9	0.994
Linalool (7)	908±40	2.8±1	0.997	11	216±10	2.3±0.5	0.998
Jasmone (8)	**1025±56**	1.7±1	0.995	**9.3**	244±23	1.3±1	0.992
Rose oxide (9)	**1100±63**	3.1±1	0.994	**9.9**	258±16	2.3±0.6	0.997
Bergapten (10)	**1181±68**	2.3±1	0.997	**8.7**	296±28	2.2±0.9	0.993
Nerol	1368±73	2.3±1	0.995	7.9	316±35	1.3±1	0.990
Geraniol (11)	1481±34	2.2±0.6	0.9991	7.3	368±12	2.4±0.3	0.9991
t-Anethole (12)	1663±54	1.3±0.8	0.998	5.9	426±13	2.0±0.3	0.9992
Citronellal (13)	2588±9	2.67±0.08	0.99998	5.7	642±3	2.74±0.04	0.99998
Citronellol (14)	2993±186	3.1±1	0.993	5.6	649±104	1.3±2	0.98
p-Cymene (15)	4445±54	2.5±0.3	0.9997	4.3	1118±10	2.80±0.08	0.99993
Limonene (16)	13175±492	5.2±0.6	0.9988	5.8	3721±1238	5.8±2	0.94

PM refers to the partition model and AM to the solute–micelle association model. Errors delimit confidence intervals, estimated at 95% CL ($n-2=15$, $t_{crit}=3.13$); r^2 is the coefficient of determination. Opt refers to the optimal SDS concentration for best resolution, calculated according to Eq. (10) in Ref. [10]. **V** was 0.246 l mol^{-1}. For estimation of μ_{MC}^{ep} it was used the empirical approximation ($\mu_{MC}^{ep}=-3.07\times10^{-3}\ C_{SDS}$ (mol l^{-1})-4.59×10^{-4}, $r^2=0.92$). For discussion on the highlighted data see text.

CMC. Indeed the mathematical fitting of the solute effective mobility and experimental data was increasingly better when N tended to infinity and CMC approached zero. However, since this mathematical artifact has no physical meaning, new calculations were conducted, where K_m/N and CMC for each solute were adjusted. The best fittings generated the K_m/N and corresponding CMC compiled in Table 1.

A limitation of this approach is that actual values of the equilibrium constant for each solute, K_m, are never known, unless N can be estimated a priori. An interesting finding reported recently in the literature by Quina et al. [21] predicts that sodium dodecylsulfate micelles are expected to grow as a power law of the total counterion salt concentration, Y_{aq}, in the aqueous phase as follows: $N=162(Y_{aq})^{1/4}$. Computing the sodium content of the electrolyte used in this work, a total sodium concentration of 60 mmol l^{-1} is obtained (40 mmol l^{-1} from tetraborate and 20 mmol l^{-1} from SDS). Therefore, a maximum aggregation number of about 80 is expected. If new calculations are computed using non-linear regression of the solute–micelle association model, with N fixed in 80 for the entire range of solutes, both fittings of K_m and CMC are not affected in any relevant manner (not shown). This result implies that 80 monomers of surfactant per micelle is a good estimate for N and consequently, true K_m values can be derived.

The individual values of CMC generated by both the partition and the solute–micelle association models were plotted against solute identity as depicted in Fig. 1. As observed, all CMC values regardless the model of origin seem to be scattered around an average value of 2.4±1, indicating no particular bias, except perhaps for coumarin and limonene, the most hydrophilic and hydrophobic compounds, respectively. This scattering around an average CMC value also suggests that despite the range of hydrophobicity of the selected solutes, no micellization seemed to be preferentially induced.

With the knowledge of CMC and N, the validity of the assumption used in the derivation of Eq. (6) can be checked, i.e., $[M] \gg [SM]$. Considering a CMC of 2.4 mmol l^{-1} and N of 80, a ratio of about 5–10 micelles per solute is expected in the interval

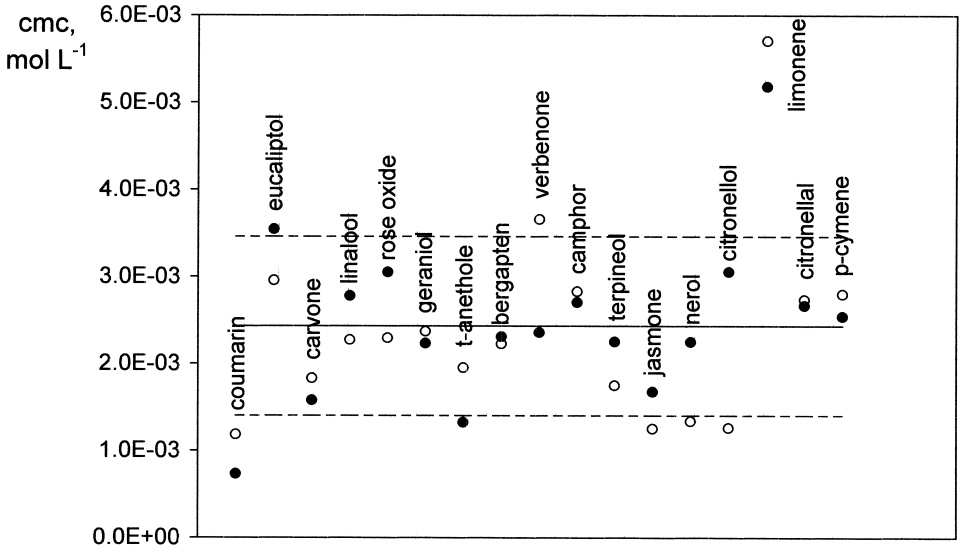

Fig. 1. CMC values adjusted individually for each solute using partition (filled symbols) and solute–micelle association (blank symbols) models. Full line represents the overall average CMC; dotted lines are CMC$\pm\sigma$ (σ is the estimate standard deviation).

of 10–40 mmol l^{-1} SDS (solute concentration is in the order of 10^{-5} mol l^{-1}). Therefore, the concentration of uncomplexed micelles is much larger than the micelles complexed by the solute, validating the assertion.

4.2. Experimental determination of the critical micelle concentration

In order to investigate further the meaning of the range of CMC estimated by the partition and solute–micelle association models, CMC was determined experimentally. Migration time of anthracene and methanol in electrolytes composed of a fixed concentration of tetraborate and increasing amounts of SDS were recorded. Three data sets of independently prepared solutions, acquired at different days with fresh buffer preparations were generated. Anthracene effective mobility was plotted against SDS analytical concentration (Fig. 2).

The effective mobility curve as a function of surfactant concentration is sigmoidal and presents two inflection points [17,22,23]. The first one referred as the critical aggregation concentration, cac, is the concentration at which surfactant monomers start to form aggregates. As the concentration of surfactant increases, the size of the aggregates increases to the point where larger well-defined structures are stabilized. The concentration at the second inflection point is termed c_2, and it is associated to the presence of free micelles. Therefore, micellization of a given surfactant is thought to occur over a range of concentrations, i.e., CMC values are larger than cac but smaller than c_2.

In order to determine CMC from a curve such as that depicted in Fig. 2, it is necessary to fit this curve to both premicellar and micellar concentration regions. However, due to a strong curvature of the mobility curve at very low SDS concentrations (data points were highlighted for clarity), it was not possible to obtain accurately an estimation of the cac value. Nevertheless, the projection of the tendency line towards zero mobility (disregarding the highlighted data points) gives us an estimation of cac of approximately 0.74 mmol l^{-1}. The intersection between the two linear segments depicted in Fig. 2 give us an estimation of c_2 concentration of 1.85 mmol l^{-1}. Therefore, the experimental CMC of SDS as determined by anthracene must be comprised between 0.74 and 1.85 mmol l^{-1}. The average CMC value obtained for all solutes during the non-linear regression fitting of both partition and solute–micelle association models, 2.4±1 mmol l^{-1}, is therefore

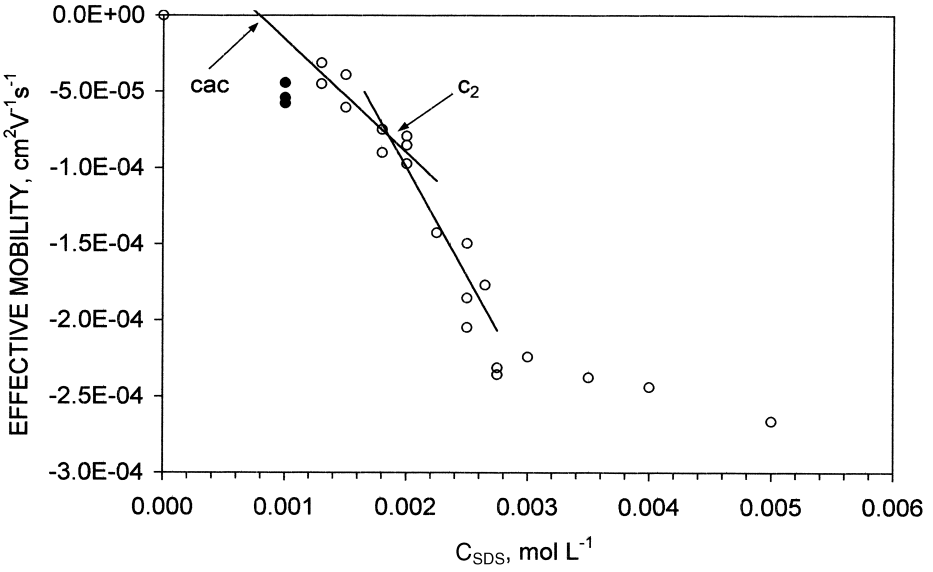

Fig. 2. Experimental determination of the critical micelle concentration of SDS. Reference marker: anthracene. Conditions: 20 mmol l^{-1} tetraborate buffer at pH 9.4, containing varying amounts of SDS; applied voltage, 20 kV; injection, 3 s, 10 mBar; detection, 200 nm. For explanation on the filled symbols see text.

within the considered error, in good agreement with the range of CMC determined experimentally with anthracene.

It is interesting to mention that the data points at very low SDS concentration (0.75 mmol l^{-1}) are not mere injection repetitions but they result from different solute solution and buffer solution preparations. Nevertheless, the effective mobility at low SDS concentration is higher (negative direction) than predicted by the tendency line. A possible explanation for this behavior relies on the inaccuracy with which measurements of retention time of anthracene at low SDS concentration are obtained. Considering that anthracene is a very hydrophobic compound, its solubility in the buffer decreases dramatically in the presence of little SDS. In fact, at low SDS concentration, it presents a distorted broaden peak, making difficult the correct assignment of its retention time. Therefore these data points (acquired at 0.75 mmol l^{-1} SDS) might be in error and were disregarded in the computation of CMC.

Another explanation for the behavior at the premicellization stage is based on the speculation that in the proximity of 0.75 mmol l^{-1} SDS a plateau is delineated. Due to the large hydrophobicity of anthracene and its poor solubility in the aqueous electrolyte medium, zero mobility is not actually feasible. Therefore, by increasing gradually the SDS concentration in the electrolyte, the solute will rapidly capture a certain number of monomers. Its effective mobility thus increases abruptly from zero to reach the mobility dictated by that plateau. From that point on, the behavior should be much alike to that described previously for other solutes, where a cac and a c_2 inflection points are defined, only that cac will be delayed.

4.3. Validation of the models

In Fig. 3 the retention factor (Fig. 3A and its expanded view Fig. 3B) and effective mobility (Fig. 3C and its expanded view Fig. 3D) of all solutes under investigation as a function of the analytical concentration of SDS are depicted. The lines were calculated from the P_{wm} and K_m computed in Table 1, using Eqs. (2) and (6), respectively, whereas the symbols represent experimental data points. In Fig. 3A,B, full lines parallel to the x-axis corresponding to retention factors of 0.5 and 20 were drawn. As commonly accepted in the practice of liquid chroma-

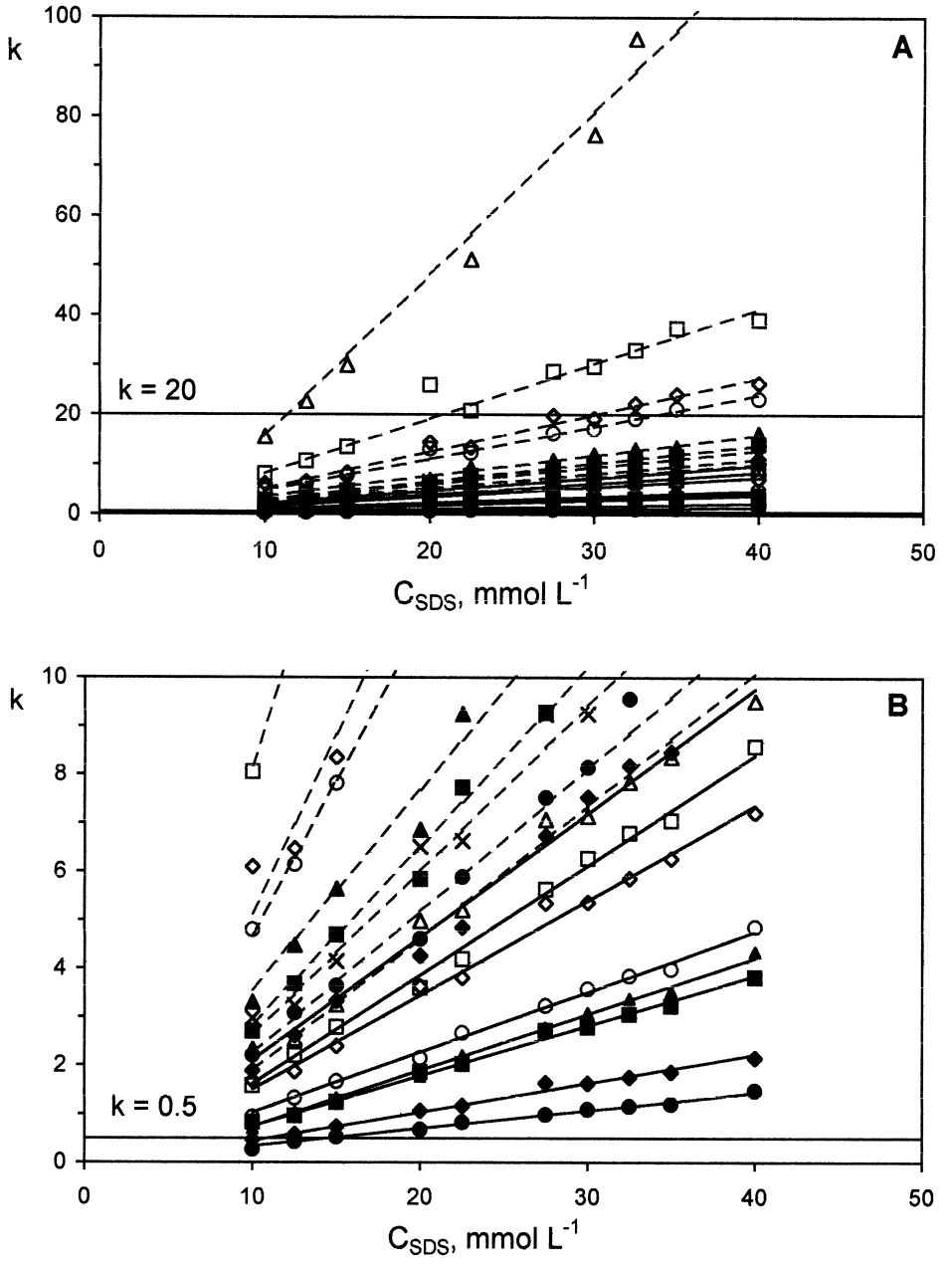

Fig. 3. Solute retention factor (A,B) and effective mobility (C,D) as a function of analytical concentration of SDS. Lines represent fitting curves; symbols represent experimental data. Full lines: Coumarin (●), Verbenone (♦), Camphor (■), Eucaliptol (▲), Carvone (○), α-Terpineol (◇), Linalool (□) and Jasmone (△). Dashed lines: Bergapten (●), Rose oxide (♦), Geraniol (■), *t*-Anethole (▲), Citronellal (○), Citronellol (◇), *p*-Cymene (□), Limonene (△) and Nerol (×). Electrophoretic conditions as in Fig. 2.

tography, retention is first optimized by adjusting conditions in such way that the retention factor falls within these limiting values. Theoretically, retention factors varied from zero to a limiting value at high surfactant concentration, where the solute retention time, t_R, approaches t_{MC}.

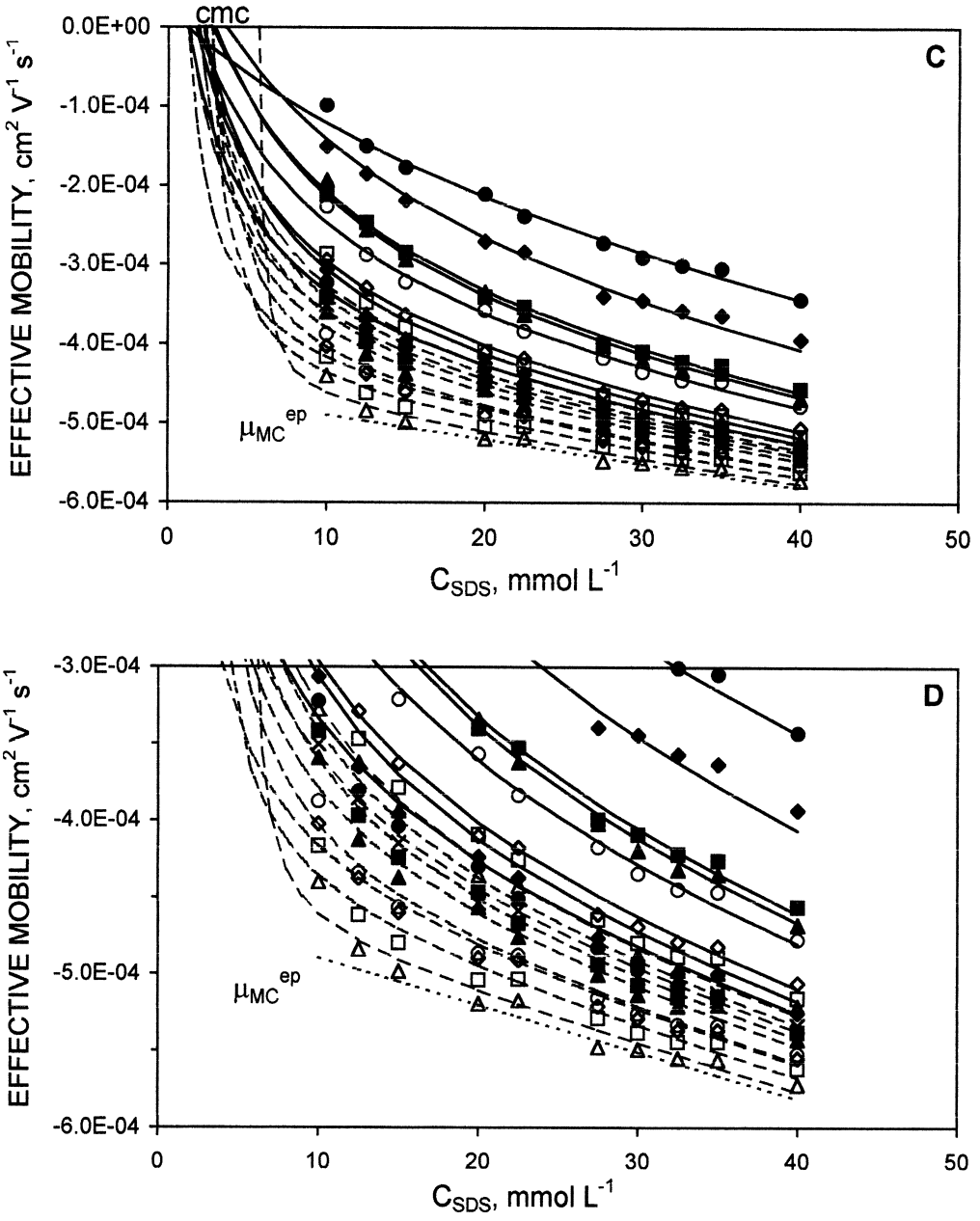

Fig. 3. (*continued*)

In Fig. 3C,D the effective mobility curves were extrapolated to lower SDS concentrations showing that theoretically, all curves must converge to the solute corresponding CMC value. Before CMC, the effective mobility approaches zero. On the same token, at high surfactant concentrations, all curves must converge to the micelle electrophoretic mobility. The mobility of the micelle (marked by anthracene) is drawn as a dotted line close to the *x*-axis. Even though mobilities are known to vary with the

square root of ionic strength (actually $\sqrt{I}/(1+\sqrt{I})$) according to Onsager equation (see Ref. [24]), in the interval from 10 to 40 mmol l^{-1} SDS, the micelle mobility was approximated by a direct linear relationship with SDS analytical concentration. Of course this approach is restricted to the SDS interval mentioned above, and it will fail to predict micelle mobility at smaller SDS concentrations. That is why experimental data and predicted line seem to lack fitting at low SDS concentration. For the most hydrophobic compounds, as it is the case of limonene, the effective mobility falls abruptly to reach the electrophoretic mobility of the micelle, whereas for more hydrophilic compounds, as it is the case of coumarin, the effective mobility approaches the micelle mobility much more gradually.

Foley in 1990 approached the optimization of micellar electrokinetic chromatographic separations by introducing an equation with which an optimal surfactant concentration could be estimated to achieve resolution between solutes of similar retention characteristics (Eq. (10) in Ref. [10]). Values of optimal concentration of surfactant for all solutes were computed using the estimated P_{wm} values and Foley equation. The results were compiled in Table 1. As indicated by the C_{SDS}^{opt}, the more hydrophobic in character is the compound, the lower the SDS concentration required for its optimal separation from an adjacent solute of similar hydrophobicity.

If ratios of the difference between individual P_{wm} to the average value are computed for solutes eluting adjacently, critical pairs can be revealed. In Table 1, solutes of similar ratios and therefore, those most likely to co-elute, were highlighted. According to this simple approach, the pair eucalyptol–carvone and the solutes jasmone, rose oxide and bergapten are the most difficult solutes to separate (P_{wm} ratios of 0.07). For jasmone, rose oxide and bergapten, a SDS concentration of about 9.5 mmol l^{-1} would be recommended for their optimal separation. However, since the retention characteristics of these solutes, especially rose oxide and jasmone are quite similar throughout the entire concentration range, complete resolution of this solute pair is unlikely to be achieved by manipulation of the SDS concentration. Moreover, as Fig. 3B illustrates, only SDS concentrations above ca. 15 mmol l^{-1} would give retention factors larger than 0.5. Therefore, the separation of eucalyptol and carvone was next considered. In this case, an optimal surfactant concentration between 17 and 20 mmol l^{-1} is recommended. It is worth mentioning that the concentration interval that comprises $0.5<k<20$ is rather limited. In order to observe the upper limiting value of 20, surfactant concentrations less than 30 mmol l^{-1} are required. At that concentration level, the three most hydrophobic compounds, limonene, *p*-cymene and citronellol, have already been excluded from the optimization strategy.

Fig. 4 presents the separation of a mixture of plant secondary metabolites under the optimal condition (20 mmol l^{-1} tetraborate buffer at pH 9.4, containing 20 mmol l^{-1} SDS). Baseline resolution of eucalyptol and carvone was achieved as anticipated by the Foley approach. Unexpectedly, rose oxide separated from jasmone but co-eluted partially with bergapten.

Table 2 contrasts the retention time of each solute as predicted by both partition and solute–micelle association models and the experimental data. For the calculation of migration time, experimental values of t_0 and t_{MC} from the electropherogram of Fig. 4 were used. The determination of t_0 is dubious due to the perturbations around the solvent band [25]; small variations of t_0 make the estimate error in t_R to vary quite a lot, including changing direction. As observed retention time can only be predicted within a relative error of ca. 8%, with larger errors associated to the most hydrophilic compounds. Even though the relative standard deviation associated with the estimation of K_m is somehow larger than that associated with P_{wm} (Table 1), the prediction of retention time using the solute–micelle association model is overall in better agreement with the experimental data (Table 2).

4.4. Applications

Fig. 5 illustrates applications of the optimization protocol to samples of essential oils. Linalool, rose oxide and caryophyllene as minor components and geraniol and citronellol as major components were identified in rose oil and geranium oil. In anise oil, a large concentration of *t*-anethole was found. Peak identity was performed by spiking techniques and on-line spectral comparisons. Peak purity check resulted in indexes greater than 900.

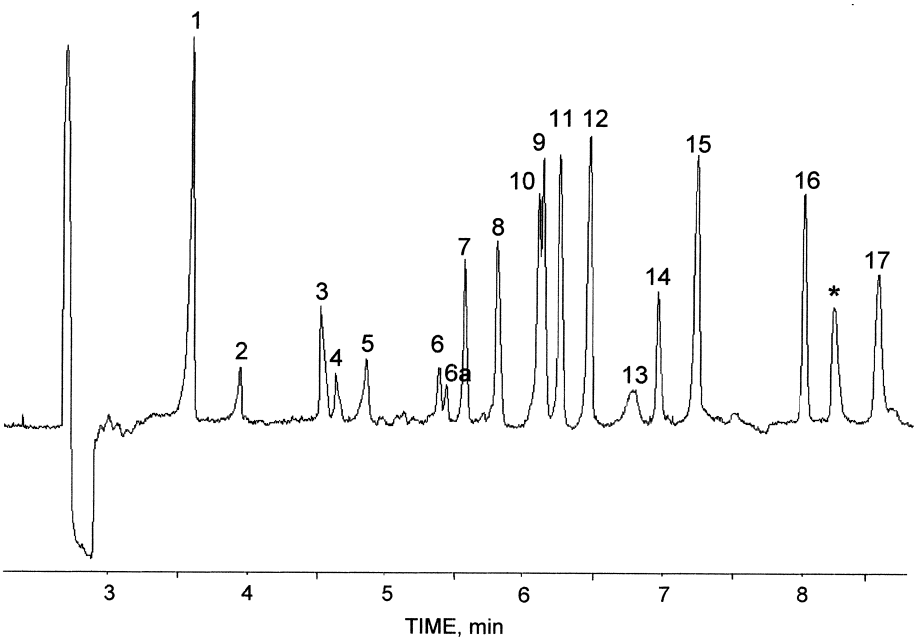

Fig. 4. Experimental validation of the optimization protocol. Separation of a mixture of plant secondary metabolite standards (100 mg l^{-1} each). Conditions: 20 mmol l^{-1} tetraborate buffer at pH 9.4, containing 20 mmol l^{-1} SDS; applied voltage 20 kV; injection 3 s, 10 mBar, detection 200 nm. Peak label as in Table 1, (6a) impurity from α-terpineol, (17) caryophyllene and (*) anthracene.

Table 2
Self-consistency test for retention time

Solute (retention order)	Retention time (min)		Retention time (min), expt.	Relative error (%)	
	Predicted			P_{wm} model	K_m model
	P_{wm}	K_m			
Coumarin	3.92	3.85	3.61	8.0	−6.2
Verbenone	4.29	4.19	3.95	7.9	−5.8
Camphor	4.91	4.73	4.53	7.8	−4.3
Eucalyptol	4.99	4.80	4.64	7.1	−3.3
Carvone	5.22	5.01	4.86	7.0	−3.0
α-Terpineol	5.78	5.47	5.38	6.8	−1.6
Linalool	5.92	5.61	5.56	6.1	−0.8
Jasmone	6.16	5.80	5.80	5.9	0.0
Rose oxide	6.15	5.79	6.13	0.8	5.7
Bergapten	6.29	5.94	6.10	2.6	2.6
Geraniol	6.56	6.14	6.25	4.7	1.7
t-Anethole	6.74	6.30	6.46	4.1	2.6
Citronellal	7.09	6.58	6.77	4.5	2.8
Citronellol	7.19	6.65	6.95	3.3	4.6
p-Cymene	7.48	6.91	7.24	3.3	4.8
Limonene	7.87	7.24	8.00	−1.7	11

Experimental conditions: 20 mmol l^{-1} tetraborate buffer at pH 9.4, containing 20 mmol l^{-1} SDS; applied voltage, 20 kV; injection, 3 s, 10 mbar; detection, 200 nm; $t_0 = 2.877$ min; $t_{MC} = 8.164$ min; total length, 58.5 cm; effective length, 50.0 cm.

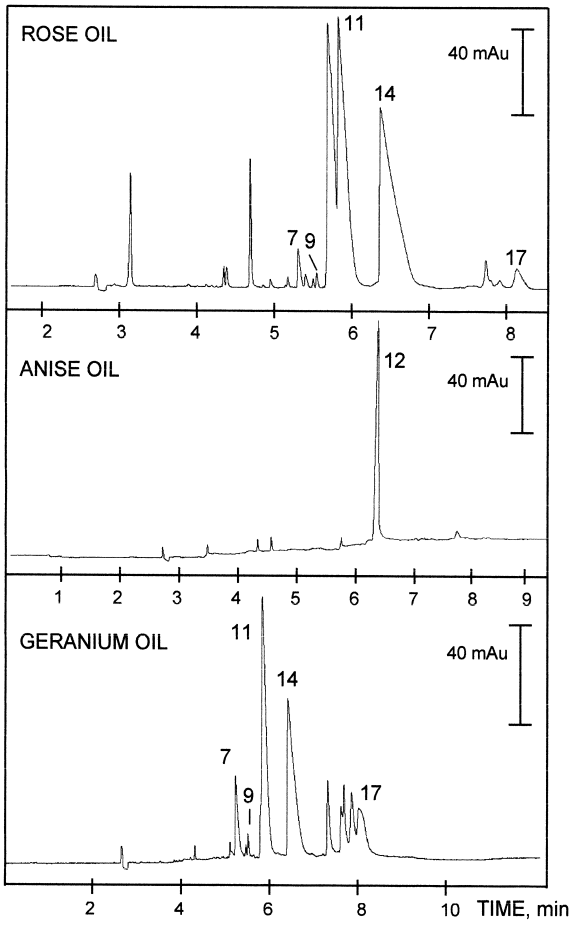

Fig. 5. Application of the optimization protocol for the analysis of essential oils. Samples were diluted 1:100 in ethanol. Conditions: 20 mmol l^{-1} tetraborate buffer at pH 9.4, containing 15 mmol l^{-1} SDS, except for anise (20 mmol l^{-1} SDS); applied voltage, 20 kV; injection, 3 s, 10 mBar; detection, 200 nm. Peak label as in Table 1 and Fig. 4.

5. Conclusions

The availability of solute–micelle interaction parameters makes possible to assess MEKC separations from a theoretical perspective. This work contributes to the literature data base with a set of partition coefficients and solute–micelle association constants for 17 plant secondary metabolites. The use of partition coefficients to predict optimal SDS concentration was experimentally validated for a standard mixture of these metabolites and applied successfully to their qualitative inspection in essential oil samples.

Acknowledgements

The authors wish to acknowledge the Conselho Nacional de Desenvolvimento Científico e Tecnológico (CNPq) and the Fundação de Amparo à Pesquisa do Estado de São Paulo (FAPESP) of Brazil for financial support (FAPESP 00/04414-4) and fellowships (CNPq 301201/94-3). Special thanks are due to Nestor Pinto Neto and Levi de Oliveira Jr. of Farma Service Indústria Farmacêutica Ltda, who kindly donated the essential oil samples. The authors are grateful to Dr. Luis Gustavo Dias for helpful discussions.

References

[1] S. Terabe, K. Otsuka, K. Ichikawa, A. Tsuchiya, T. Ando, Anal. Chem. 56 (1984) 111.
[2] H. Nishi, S. Terabe, J. Chromatogr. A 735 (1996) 3.
[3] M.G. Khaledi, J. Chromatogr. A 780 (1997) 3.
[4] D. Perrett, Ann. Clin. Biochem. 36 (1999) 133.
[5] F. Tagliaro, F. Bortolotti, J. Forensic Sci. 47 (2002) 713.
[6] Z. El Rassi (Ed.), CE and CEC Reviews, Wiley, New York, 2001.
[7] G. Gübitz, M.G. Schmid, Electrophoresis 21 (2000) 4112.
[8] K.R. Nielsen, J.P. Foley, in: P. Camilleri (Ed.), Capillary Electrophoresis—Theory and Practice, 2nd edition, CRC Press, Boca Raton, FL, 1998, p. 135.
[9] J.P. Foley, Anal. Chim. Acta 231 (1990) 237.
[10] J.P. Foley, Anal. Chem. 62 (1990) 1302.
[11] A.S. Kord, J.K. Strasters, M.G. Khaledi, Anal. Chim. Acta 246 (1991) 131.
[12] M.G. Khaledi, S.C. Smith, J.C. Strasters, Anal. Chem. 63 (1991) 1820.
[13] J.K. Strasters, M.G. Khaledi, Anal. Chem. 63 (1991) 2503.
[14] M.A. García, M.L. Marina, J.C. Díez-Masa, J. Chromatogr. A 732 (1996) 345.
[15] M.A. García, J.C. Díez-Masa, M.L. Marina, J. Chromatogr. A 742 (1996) 251.
[16] A.B. Prevot, E. Pramauro, M. Gallarate, M.E. Carlotti, G. Orio, Anal. Chim. Acta 412 (2000) 141.
[17] C.-E. Lin, K.-S. Lin, J. Chromatogr. A 868 (2000) 313.
[18] N.G. Bisset, M. Wichrl (Eds.), Herbal Drugs and Phytopharmaceuticals, CRC Press, Boca Raton, FL, 2001.
[19] W.L. Hinze, D.W. Armstrong (Eds.), Ordered Media in Chemical Separations, American Chemical Society, Washington, DC, 1987.

[20] A. Berthod, C.G. Alvarez-Coque, in: Micellar Liquid Chromatography, Marcel Dekker, New York, 2000.
[21] F.H. Quina, P.M. Nasser, J.B.S. Bonilha, B.L. Bales, J. Phys. Chem. 99 (1995) 17028.
[22] C.-E. Lin, M.-J. Chen, H.-C. Huang, H.-W. Chen, J. Chromatogr. A 924 (2001) 83.
[23] J.C. Jacquier, P.L. Desbène, J. Chromatogr. A 718 (1995) 167.
[24] R.A. Robinson, R.H. Stokes, in: Electrolyte solutions—The Measurement and Interpretation of Conductance, Chemical Potential and Diffusion in Solutions of Simple Electrolytes, Butterworths, London, 1959.
[25] E.S. Ahuja, R.L. Little, J.P. Foley, J. Liq. Chromatogr. 15 (1992) 1099.